Developmental Biology 325 (2009) 273–280

Contents lists available at ScienceDirect

Developmental Biology

journal homepage: www.elsevier.com/developmentalbiology

Shh and ROCK1 modulate the dynamic epithelial morphogenesis in circumvallate papilla development

Jae-Young Kim [a], Min-Jung Lee [b], Kyoung-Won Cho [b], Jong-Min Lee [b], Yeun-Jung Kim [b], Ji-Youn Kim [b], Hye-In Jung [a], Je-Yoel Cho [a], Sung-Won Cho [b], Han-Sung Jung [b,*]

[a] Department of Biochemistry, School of Dentistry, Brain Korea 21 project, IHBR, Kyungpook National University, Daegu, Republic of Korea
[b] Division in Anatomy and Developmental Biology, Department of Oral Biology, Research Center for Orofacial Hard Tissue Regeneration, Brain Korea 21 project, Oral Science Research Center, College of Dentistry, Yonsei Center of Biotechnology, Yonsei University, 134 Shinchon-Dong, Seodaemoon-Gu, Seoul, 120-752, Republic of Korea

ARTICLE INFO

Article history:
Received for publication 5 June 2008
Revised 23 October 2008
Accepted 25 October 2008
Available online 5 November 2008

Keywords:
Circumvallate papilla
ROCK1
Wnt11
Shh
Cytoskeleton
Proliferation

ABSTRACT

In rodents, a circumvallate papilla (CVP) develops with dynamic changes in epithelial morphogenesis during early tongue development. Molecular and cellular studies of CVP development revealed that there would be two different mechanisms in the apex and the trench wall forming regions with specific expression patterns of *Wnt11* and *Shh*. Molecular interactions were examined using *in vitro* organ culture with over-expression of Shh, important signalling molecules and various inhibitors revealed that there are two significant different mechanisms in CVP formation by *Wnt11* and *Shh* expressions. Wnt, a well known key molecule to initiate taste papillae, would govern Rho activation and cytoskeleton formation in the apex epithelium of CVP. In contrast, *Shh* regulates the cell proliferation to differentiate taste buds and to invaginate the epithelium for development of von Ebner's gland (VEG). Based on these results, we suggest that these different molecular signalling cascades of Wnt11 and Shh would play crucial roles in specific morphogenesis and pattern formation of CVP during early mouse embryo development.

Introduction

Gustatory papillae are one of the specialized and complex structures, which posses taste buds, found on the dorsal surface of the tongue. There are three types of gustatory papillae in mammals on the tongue surface. The fungiform papillae are distributed on the anterior two-thirds of the tongue, the foliate papillae are found at both lateral sides of posterior one-third of tongue, and the circumvallate papilla is found in the posterior one-third of the tongue in rodents. Circumvallate papilla (CVP) is an unique organ, developing on two-thirds of a tongue dorsal surface from the anterior part (Lee et al., 2006). Initiation of CVP morphogenesis, epithelial thickening, followed by invaginations of the epithelia into the underlying mesenchyme, share similar processes in the development of other epithelial appendages such as feather, hair, and tooth (Pispa and Thesleff, 2003). In addition, CVP contains taste buds only in the trench wall epithelium with specific patterning. These taste buds contain sensory cells for the chemical sense of taste and require nerve innervations to convey sensory information to the central nervous system. However, the molecular mechanisms that govern the patterning of taste buds in CVP and the morphogenesis of CVP itself are not well understood. Interestingly, in previous reports, specific localizations of cellular markers and expression patterns of genes in CVP development suggested that there would be specific molecular mechanisms for CVP morphogenesis and pattern formation of taste buds in CVP (Jitpukdeebodintra et al., 2002; Lee et al., 2006).

Shh expression is involved in the induction and morphogenesis of early CVP and salivary gland development (Jaskoll et al., 2004). The intensity of *Shh* expressions appear to increase in the epithelium of the lateral trench wall (where taste buds eventually form) and also in the von Ebner's gland (VEG)-forming area in early development (Lee et al., 2006). *Shh* also has been observed to play important roles in several fundamental developmental processes, including the initiation, determination and differentiation of fungiform papillae (Chuong et al., 2000; Kim et al., 2005a, 2003). In addition, *Shh* is well known as an important mitogenic factor during the development of neural tube, kidney and prostate gland (Lamm et al., 2002; Thibert et al., 2003; Yu et al., 2002).

Wnts are secreted factors involved in patterning, tissue polarity, and cell fate specification in many developing systems (Dale, 1998; Huelsken and Birchmeier, 2001). *Wnt* genes are the vertebrate homologues of wingless (wg) in *Drosophila*, and in vertebrates that they form a large gene family (Nusse and Varmus, 1992). Wnts transmit their signal through at least three distinct intracellular pathways. One, the so-called canonical pathway, involves translocation of β-catenin to the cell nucleus. The others involve, respectively, release of intracellular Ca^{2+} and activation of RhoA, which leads to effects on the actin cytoskeleton and on planar polarity (Dale, 1998; Huelsken and Birchmeier, 2001; Kuhl et al., 2000). The choice of

* Corresponding author. Fax: +82 2 312 8012.
E-mail address: hsjung@yuhs.ac (H.-S. Jung).

0012-1606/$ – see front matter © 2008 Elsevier Inc. All rights reserved.
doi:10.1016/j.ydbio.2008.10.034

pathway is dependent on the characteristics of the receptors, called Frizzled (Fz) proteins that are members, like the Wnt proteins, of a large family. Wnt proteins bind preferentially to certain Frizzled receptors (He et al., 1997). In addition, certain Fz receptors signal preferentially through either the β-catenin, RhoA, or $Ca2^+$ pathways (Hartmann and Tabin, 2000). Non-canonical Wnts, including Wnt-4, -5a, -11, can activate the Wnt/PCP pathway, which in *Drosophila* regulates planar cell polarity (PCP) leading to the formation of polarized tissues. In both canonical and non-canonical Wnt pathways, Fz receptors and the intracellular scaffold protein Dishevelled (Dsh) are critical for signal transduction.

However, in the non-canonical Wnt pathway Dsh is trans-located to the plasma membrane where it interacts with a different set of effector proteins (Axelrod et al., 1998). Dsh activates small GTPases such as RhoA, CDC42 and Rac, which in turn activate Rho-associated kinase (ROCK) and c-Jun N-terminal kinase (JNK) modulating tissue separation, cell adhesion, process formation and cytoskeletal rearrangements (Choi and Han, 2002; Habas et al., 2003; Winklbauer et al., 2001). Rho kinases (ROCKs) are protein serine/threonine kinases and are downstream effector molecules of Rho (Keller et al., 2002). Although ROCK has been demonstrated to play an important role in heart and brain development as well as in neural tube formation, the role of ROCK in the morphogenesis of epithelial organs such as the embryonic CVP remains to be fully elucidated (Meyer et al., 2006).

In this study, rolling *in vitro* organ culture system was employed to elucidate the precise molecular mechanisms of *Shh* and *Wnt11*. Especially we carefully examined the Shh pathway that would involve in pattern formation and proliferation of epithelial cells on the surface of the developing mouse tongue. In addition, we examined the *Wnt11* pathway that activates of RhoA, which leads to effects on the actin cytoskeleton to form a specific morphogenesis of CVP. Dynamic morphological changes with specific gene regulations would refer that confined CVP development is strictly associated *Shh* and *Wnt11*.

Materials and methods

All experiments were performed according to the guidelines of the Yonsei University, College of Dentistry, Intramural Animal Use and Care Committee.

Animals

Adult ICR mice were housed in a temperature-controlled room (22 °C) under artificial illumination (lights on from 05:00 to 17:00), at 55% relative humidity, with free access to food and water. Mouse embryos were obtained from time-mated pregnant mice. The day on which a vaginal plug was confirmed then designated as embryonic day 0 (E0).

In vitro organ culture with pharmacological inhibitors

In order to determine the regulation of the signaling molecules after micro-dissecting the tongue from an E13.5 mouse mandible, the tongues were separated into its aboral and oral regions (Kim et al., 2003). They were then cultured in a medium containing 10% fetal bovine serum for 2 days according to the method described previously (Shiota et al., 1990). Briefly, explanted tongues were cultivated in a 50-ml penicillin bottle containing 8 ml of the culture medium, which had been sterile-filtered. Three or four explants were put into one bottle, and the bottle was sealed airtight with a rubber stopper and a metal clamp. The bottles were flushed for approximately 2 min with a gas mixture of 50% O_2, 45% N_2, and 5% CO_2. The bottles were incubated at 37 °C on a roller device (20 rpm) for 48 h. The culture bottles were flushed every 24 h with the same gas mixture. Inhibitor of Rho kinase (Y27632) from Calbiochem (San Diego, CA) and 5E1, Anti-SHH-antibody (Hybridomabank, USA) were treated during cultivation.

Di.I. micro-injection

Di.I. (Molecular Probes, Eugene, OR, USA) is a vital, highly fluorescent, lipophilic dye belonging to the carbocyanine dye family. After Di.I. micro-injection into designated regions of the CVP epithelium, the migration pattern of Di.I.-labeled cells was observed at 48 h by using fluorescence microscopy (MZ-FLIII; LEICA, Jena, Germany).

DNA electroporation

Plasmid DNA was purified by using a plasmid purification kit (Qiagen, Valencia, CA, USA) and dissolved in T1/4E (10 mM Tris–HCl, pH 8.0/0.25 mM EDTA). Fast Green at 1/10,000 (Sigma, USA) was added to the DNA solution for visualization within the tissue. A micro-capillary needle was used to inject ~1 μg/μl DNA into the CVP forming region, after which 20-ms current pulses of 25 V were applied with an electroporator. The experimental group comprised the CVP region electroporated with Shh in pEGFP-N1 or Shh in pIRES-DsRed construct. The other tongue was electroporated with constructs containing only fluorescent proteins (EGFP and DsRed) and used as controls.

Histology and immunohistochemistry

Sections were routinely stained with hematoxylin and eosin (HE) and evaluated by microscopy. Specimens were fixed in 4% paraformaldehyde (PFA) in phosphate-buffered saline (PBS) overnight at 4 °C, embedded in paraffin wax using conventional methods and then cut to a thickness of 7 μm. The tissue sections were then dewaxed and rehydrated. In order to reduce non-specific background staining attributable to endogenous peroxidase activity, slides were incubated in 0.3% hydrogen peroxide for 15 min. The tissue sections were boiled in 10 mM citrate buffer (pH 6.0) for 10 min followed by cooling at 25 °C for 20 min. To reduce the non-specific binding while using mouse monoclonal antibody to mouse tissue, we used blocking solution for 65 min (Labvision, USA, cat. no. TQ-015-HD; Ultra V block for 5 min, Rodent block for 60 min). Sections were incubated with mouse monoclonal antibody against ROCK1 (EP786Y; Abcam, USA; cat. no. ab45171) or Rabbit monoclonal antibody against Ki67 (SP6; Neo Markers, USA; cat. no. RM-9106) as the primary antibody at 4 °C overnight. After being washed for 10 min in PBS, the Ki 67 specimens were then incubated with biotinylated goat anti-mouse and rabbit immunoglobulin secondary antibodies for 10 min, followed by a 10 min PBS wash and 10 min incubation in streptavidin–peroxidase at room temperature. Finally, the binding of primary antibody to the sections was visualized by using a diaminobenzidine tetrahydrochloride (DAB) reagent kit (Zymed, USA; cat. no. 00-2014). In case of ROCK1 specimens, after primary antibody incubation, were FITC labeled using mouse immunoglobulin secondary antibodies for 2 h and washed for 5 min. Then, specimens were mounted using aqueous mounting medium (Beckman Coulter, Japan, cat. no. PNIM0752). After the histological process, HE-stained CVP images were collected with a Spot RT digital camera (Leica, Germany). We used at least 10 slides to examine the shapes and sizes of CVP and trench wall in each experimental group. Width of CVP apex and depth of trench wall were measured by means of an eyepiece graticule attached to a binocular microscope. Statistical analysis of these measurements consisted of an independent *t*-test.

Actin filament-specific immunofluorescent staining

Phalloidin staining was performed according to the previous reported method (Kim et al., 2005b; Michael et al., 2005). The specimens were fixed with 4% PFA in PBS for 24 h. After embedding the specimens in paraffin, sections of 3 μm thickness were obtained. The samples were dewaxed in xylene for 10 min and rehydrated using

a graded series of ethanol. After rinsing with PBS, the tissues were treated with 5 mg/ml trypsin (GIBCO) for 30 min at 37 °C. After rinsing three times with PBS, the sections were incubated in 5 mg/ml phalloidin (Sigma, P5282) for 20 min at room temperature. The specimens were rinsed again with PBS and examined using fluorescence microscopy (LEICA, MZ FL III).

In situ hybridizations

In situ hybridization on whole mouse embryos was performed as previously described (Eblaghie et al., 2004) in wax sections by using standard protocols. Briefly, embryos were fixed in 4% PFA, embedded in paraffin wax and sectioned at 7 μm. Sections were baked at 65 °C, dewaxed in xylene, rehydrated through a graded series of alcohol washes and post-fixed in 4% PFA. Sections were prehybridized in a humid chamber containing 50% formamide in 2× saline sodium citrate buffer at 55 °C for 30 min. Digoxigenin (DIG)-labelled RNA probes were pre-warmed to 80 °C and hybridized to sections overnight at 65 °C. Mouse DNA *Shh* and *Wnt11* plasmids were used as templates for the synthesis of DIG-labeled RNA probes, as kindly provided by Dr. Y.-P. Chen (Tulane University, USA).

Results

Expression patterns of key molecules in CVP morphogenesis

In order to define the precise localizations of *Shh* and *Wnt11*, section *in situ* hybridization and immunohistochemistry were examined at E13.5 and E15.5 (Fig. 1). Since these two developmental stages show the most dramatic alterations in CVP morphogenesis, *Wnt11* expressions were examined in the epithelium of tongue dorsal area at E13.5 (Fig. 1A). At E15.5, expression patterns of *Wnt11* were examined in the epithelium of CVP forming region (Fig. 1B). Especially, apex epithelium of CVP forming region showed strong expression patterns of *Wnt11* at E15.5. At E13.5, *Shh* expressions were detected in the apical epithelium of CVP forming region (Fig. 1C). At E15.5, *Shh* showed specific expression patterns in the lateral epithelium, where taste buds and von Ebners' gland would develop later (Fig. 1D). ROCK1 localizations were also examined at E13.5 and E15.5. Strong ROCK1 localizations were detected in the apex epithelium of CVP forming region at E13.5 (Fig. 1E). At E15.5, weak ROCK1 localizations were observed in the epithelium of CVP forming region, coincided with expression patterns of *Wnt11* (Fig. 1F). In order to examine the role of cytoskeleton formation in CVP morphogenesis, actin filaments were examined at E13.5 and E15.5 by phalloidin staining. Both E13.5 and E15.5 stages showed similar staining patterns of phalloidin that apex parts of epithelium were detected with positive staining (Figs. 1G, H). Interestingly, at E15.5 phalloidin staining results showed the opposite localization pattern with that of the *Shh* expression. These specific expression patterns of molecules implied that there would be unravelled relationships between *Wnt11*/ROCK1 and *Shh* via cytoskeleton formation during CVP development.

In vitro organ culture and cell migration pattern

In order to examine the molecular mechanisms in CVP development, rolling *in vitro* organ culture was employed at E13.5 (Fig. 2A). After 2 days cultivation, HE staining showed that *in vitro* organ culture of tongue demonstrated E15 morphogenesis of CVP development *in vivo* (Fig. 2B). ROCK1 localization pattern was similar to that of *in vivo,* E15.5 (Fig. 1F). ROCK1 was localized in the epithelium of CVP forming region (Fig. 2C). After a 2 day culture at E13.5, *Wnt11* expressions were detected in the apex epithelium of CVP forming region (Fig. 2D). The lateral epithelium of CVP showed strong expression patterns of *Shh*, similar to that of E15.5 (Figs. 1D and 2E). Ki67, as a marker for cell proliferations, were examined. Strong

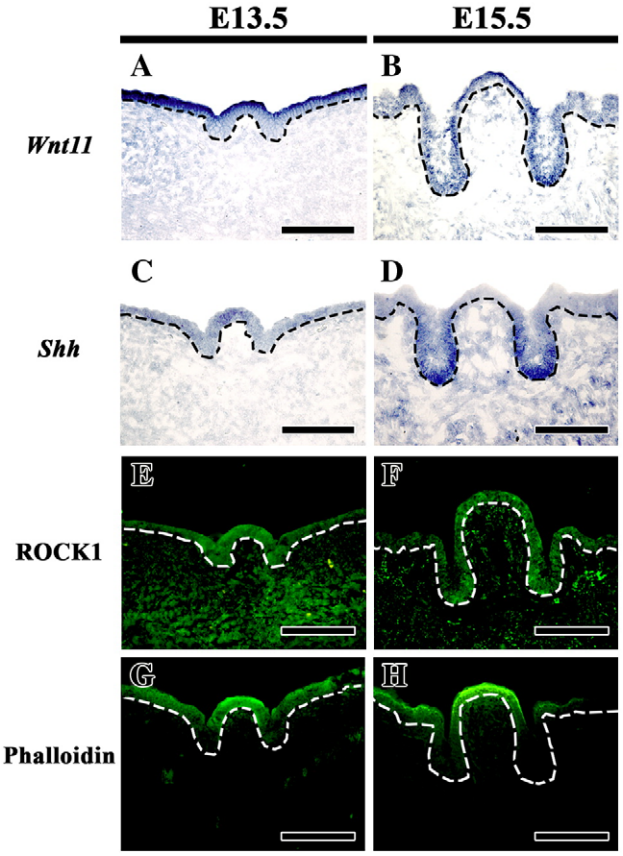

Fig. 1. Expression and localization patterns of molecules in CVP development. (A–D) Expression patterns of *Wnt11* and *Shh* in CVP development. (A) *Wnt11* expressions are detected in the epithelium at E13.5. (B) At E15.5, apex and lateral trench wall regions of epithelium show strong expression patterns of *Wnt11*. (C) *Shh* expressions are observed in the apex epithelium of CVP forming region at E13.5. (D) Strong expression patterns of *Shh* are detected in the epithelium of lateral trench wall and VEG forming region at E15.5. (E–F) Localization patterns of ROCK1 in CVP development. (E) At E13.5, ROCK1 localizations are observed in the apex epithelium of CVP forming region and in the epithelium of tongue dorsal surface. (F) At E15.5, ROCK1 localizes in the epithelium of CVP forming region. Localization pattern of ROCK1 shows similar localization patterns to *Wnt11*. (G–H) Actin filament formation are examined by phalloidin staining. (G) At E13.5, phalloidin positive staining is observed in the epithelium including CVP forming region and tongue dorsal surface. (H) At E15.5, in the epithelium of CVP forming region shows strong localization of phalloidin positive staining. Phalloidin staining results are similar to those of *Wnt11* expression pattern and ROCK1 localization pattern (all photos were taken by same magnification, black and white dotted lines demarcate basement membrane, scale bars: 100 μm).

positive localizations of Ki67 were shown in the lateral epithelium of CVP forming region (Fig. 2F). Although intensity of phalloidin staining was different from that of the E15.5, positive phalloidin staining at apex epithelium of CVP showed a similar localization pattern to that of the E15.5 (Fig. 2G). Dynamic morphological changes of CVP development is examined by Di.I. micro-injection to understand the precise epithelial cell migration patterns during CVP morphogenesis. After 2 days *in vitro* organ culture, Di.I. micro-injected epithelial cells where lateral sides of CVP forming region were not migrated into the lateral trench wall epithelium of CVP forming region (Figs. 2H–K; $n=12/12$; 100%). Di.I. micro-injections at anterior and posterior parts of CVP forming epithelium also showed that there were no migration patterns into the CVP forming region (Figs. 2L–O; $n=12/12$; 100%). The level of the anterior epithelial invaginations was much less than that of lateral epithelium of CVP forming region (Fig. 2O). After 2 days tracing, epithelial cells of the apex region of CVP were not migrated into the lateral trench wall forming epithelium (Figs. 2P–S; $n=12/12$; 100%). These obvious migration patterns suggested that epithelial invaginations in CVP

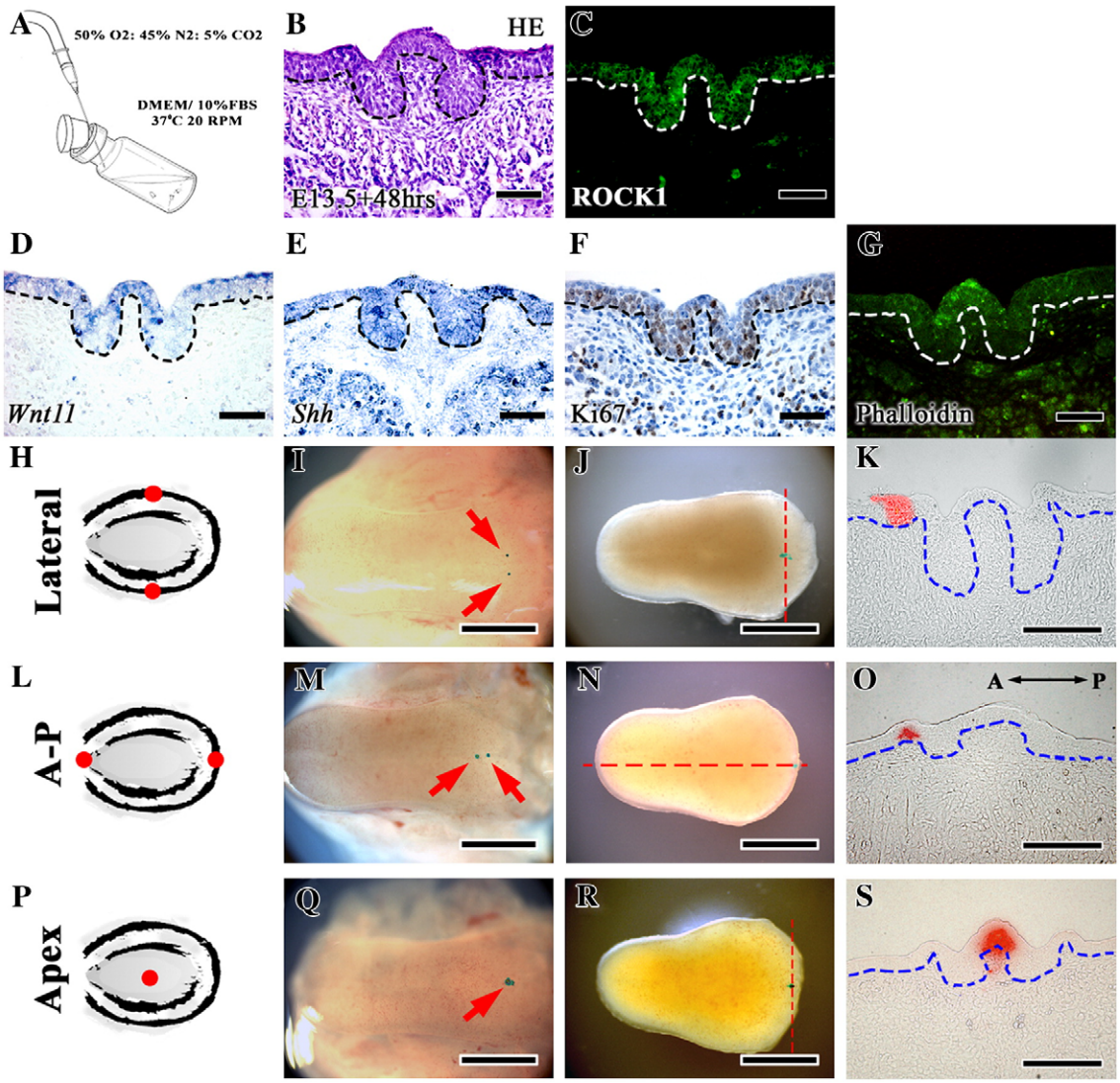

Fig. 2. *In vitro* rolling organ culture at E13.5 for 2 days. (A) Schematic diagram for *in vitro* rolling organ culture method. Explanted tongues are cultivated in a 50-ml penicillin bottle containing 8 ml of the DMEM culture medium. The bottles are flushed for approximately 2 min with a gas mixture of 50% O_2, 45% N_2, and 5% CO_2. The bottles are incubated at 37 °C on a roller device (20 rpm) for 48 h. (B–F) Morphogenesis and localization patterns of key molecules after *in vitro* rolling organ culture for 2 days. (B) HE staining shows similar morphology to E15 of CVP. (C) Strong ROCK1 localization patterns are examined apex epithelium of CVP forming region. However weak localizations are observed in tongue dorsal surface epithelium. (D) *Wnt11* expressions are detected in the apex epithelium of CVP forming region. (E) *Shh* expresses in the epithelium of VEG and lateral trench wall forming regions. (F) Ki67 positive staining is localized in the tip of invaginated epithelium. (G) Phalloidin staining shows the strong positive localizations of actin filaments in the apex epithelium of CVP forming region (B–G, scale bars: 50 μm). (H, L, P) Diagrams of Di.I. micro-injected points (red dots indicate micro-injection points). (I, M, Q) At E13.5, in order to understand the precise epithelial cell migration patterns during CVP morphogenesis, Di.I. micro-injection into the epithelium of CVP forming regions are examined (red arrows indicate the injected points). (J, N, R) After 2-day cultivation, Di.I. micro-injected cells are examined by histological sections (red dotted lines demarcate the section levels) (I, J, M, N, Q, R, scale bars: 500 μm). (K, O, S) Sections show that there are no migration patterns of micro-injected epithelial cells in CVP development (black, blue, and white dotted lines demarcate basement membrane, K, O, S, scale bars: 100 μm).

development would be a result not from cell migration but from cell proliferation.

Pharmacological inhibition of ROCK1 by Y27632

In order to examine the function of Wnt11 signalling including ROCK1 during CVP morphogenesis, rolling *in vitro* organ culture was examined with treatment of Y27632 for 2 days at E13.5. Various concentrations of Y27632 were examined with the same rolling *in vitro* organ culture conditions (data not shown). After treatments of 5, 10 and 25 μM of Y27632 we could examine the effects of Y27632 in CVP formation with the concentration dependent manner that epithelial tissues were more invaginate into the mesenchymal region at higher concentration of Y27632. Finally we could conclude that the most effective concentration would be 50 μM of Y27632, shown with the striking alterations of CVP morphogenesis (Fig. 3A; n=20/20; 100%). Apical epithelium of a CVP forming region was dramatically decreased but epithelium of a lateral epithelium region, which would be formed VEG (von Ebner's gland) later, was dramatically increased (Fig. 3A). Cell proliferations were examined by Ki67 immunostaining to define the relationship between ROCK1 signalling and epithelial cell proliferation. Intensive Ki67 positive reactions were examined in the epithelium of VEG forming region, where the tip of invaginated epithelium (Fig. 3B). ROCK1 localizations in the epithelium were decreased when compared with its control (Fig. 1C). ROCK1 localizations were detected in the epithelium of apex region and tongue dorsal surface (Fig. 3C). *Wnt11* expression patterns were examined in the epithelium of CVP forming region (Fig. 3D). Expression patterns of *Wnt11* were also examined in the tongue dorsal epithelium.[AU1] However *Shh* expression patterns were altered when compared with the control culture (Figs. 3E and 2E). Interestingly, intensity of *Shh* expression was increased in the both apex and lateral epithelium of

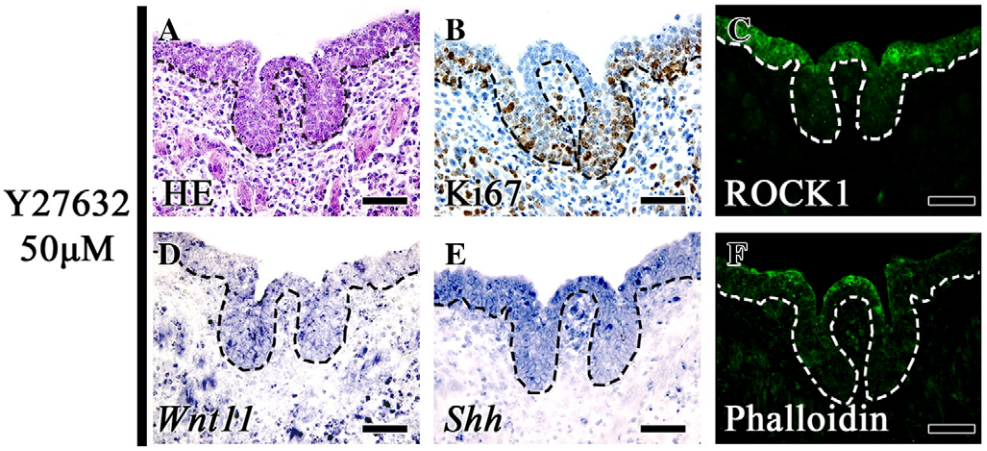

Fig. 3. Pharmacological inhibitor of ROCK1, Y27632 treatment. (A–F) At E13.5, in order to examine the effects of inhibition of Wnt signalling, 50 μm Y27632 is treated for 2 days *in vitro* rolling organ cultivation. (A) HE staining shows interesting morphological changes after 50 μm Y27632 treatment that apex epithelium is decreased but lateral trench wall epithelium is much increased. (B) Cell proliferation is examined by Ki67 immunostaining. Ki67 positive localizations are examined in the invaginated tip of CVP forming epithelium. (C) ROCK1 localizations are also much decreased in the apex epithelium of CVP forming region. However tongue dorsal epithelium shows increased localization pattern of ROCK1. (D) Expression pattern of *Wnt11* is examined in the whole epithelium including CVP forming and tongue dorsal regions. (E) *Shh* expression patterns are examined in all of the epithelium of tongue dorsal surface and CVP forming region. (F) Phalloidin staining shows much decreased intensity in the apex epithelium of CVP forming region (black and white dotted lines demarcate basement membrane, all photos were taken in same magnification, scale bar: 50 μm).

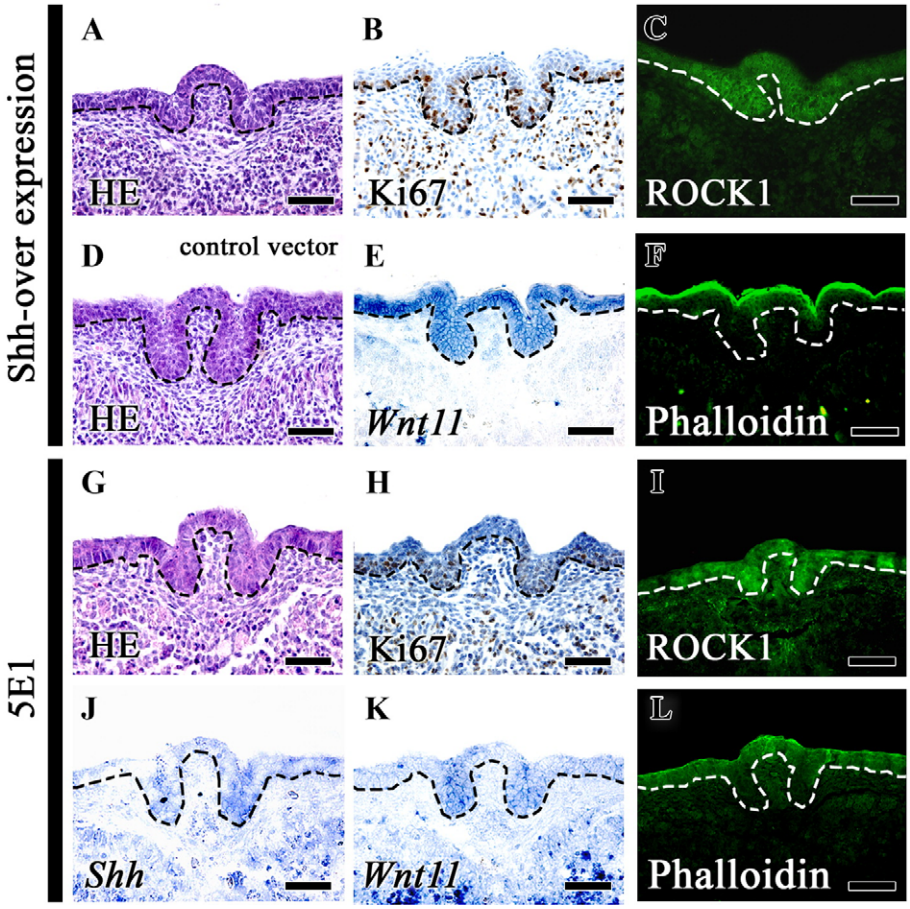

Fig. 4. Functional analysis of Shh in epithelial morphogenesis of CVP. (A–G) Shh over-expressions are examined by electroporation method. (A) HE staining shows much decreased epithelial invagination of the lateral trench wall and VEG forming regions. (D) HE staining after the control vector electroporation shows similar morphogenesis of control culture (Fig. 2B). (B) Much decreased Ki67 positive staining cells are observed in the epithelium of tongue dorsal surface and lateral trench wall forming region. (C) ROCK1 localizations are not altered when compared with control culture (Fig. 2C). (E) *Wnt11* expression is much increased and shows the broad expression pattern in the whole epithelium. (F) Phalloidin staining shows similar results to that of the control culture (Fig. 2G). (G–L) 5E1, SHH-antibody, is treated as a loss of function. (G) After 5E1 treatment, HE staining shows dramatic alterations in morphogenesis of CVP. Invagination of epithelium is much decreased after Shh blocking by 5E1 treatment. (H) Ki67 positive staining is decreased when compared with the control culture (Fig. 2F). (I) ROCK1 localizations are similar to that of the control culture. (J) Decreased expression patterns of *Shh* are examined in the epithelium. (K) *Wnt11* expressions are examined in the lateral trench wall forming epithelium. (L) Phalloidin staining result is similar to that of the control culture (Fig. 2G) (black and white dotted lines demarcate basement membrane, all photos were taken in same magnification, scale bar: 50 μm).

CVP forming region. Actin filament formations were examined by phalloidin staining (Fig. 3F). Actin filament formation, restricted in the apex epithelium of CVP forming region, was much decreased when compared with that of the control (Fig. 2G). These results suggested that cytoskeletal formation controlled by Rho kinase (ROCK) would play an important role in CVP morphogenesis. In addition, increased *Shh* expression patterns implied that one can predict an antagonistic regulation between *Shh* and ROCK1.

Functional analysis of Shh in CVP morphogenesis

In order to examine the role of *Shh* in CVP morphogenesis and pattern formation, we employed the gain of function with Shh over-expression and the loss of function with the treatment of 5E1, SHH-antibody for neutralization of *Shh*. After the Shh over-expression, morphological changes were observed by HE staining (Fig. 4A). Invagination of epithelium was decreased after the Shh-electroporation and apex epithelium of CVP was larger when compared with control vector electroporation (Figs. 4A and E; $n=18/20$; 90%). Ki67 localizations were decreased than that of the control (Fig. 4B). Ki67 positive cells were detected in the tongue dorsal and CVP forming region basal layer region of the epithelium with decreased expression patterns than that of the control (Fig. 4B). ROCK1 localizations were examined to define the relationships between *Wnt11*, ROCK1 and *Shh* in CVP formation. After treatment of 5E1, ROCK1 localization patterns were slightly increased when compared with the control culture (Fig. 4C). Expression pattern of *Wnt11* was increased in the whole epithelium including tongue dorsal and CVP forming epithelium than that of the control (Fig. 4E). Phalloidin staining after the Shh over-expression showed increased actin filament formation in the tongue dorsal and apex region of CVP forming epithelium (Fig. 4F). In contrast to apex and tongue dorsal surface, there were no positive localizations of actin filaments in the lateral trench wall forming region (Fig. 4F).

5E1, a neutralizing antibody to SHH, treatment showed the alterations in CVP morphogenesis and expression patterns of signalling molecules. HE staining showed those invaginations of epithelium to form the lateral wall and VEG (von Ebner's gland) were obviously decreased (Fig. 4G; $n=17/20$; 85%). This altered morphogenesis of CVP was similar to that of the Shh over-expression (Fig. 4A). Ki67 positive localizations were much decreased in the whole epithelium including apex, lateral and tongue dorsal epithelium (Fig. 4H). ROCK1 localizations were slightly different from both the control and Shh over-expression. Stronger localization patterns of ROCK1 were detected in the epithelium of the tongue dorsal and apex forming regions of CVP (Fig. 4I). After treatment of 5E1, *Shh* expression patterns were examined to understand the auto-regulations in Shh signalling. Expression pattern of *Shh* was not altered much after 5E1 treatment (Fig. 4J). Expression pattern of *Wnt11* was altered after 5E1 treatment. Expression of *Wnt11* was mainly detected in the lateral wall forming region of CVP (Fig. 4K). Phalloidin staining showed that active actin filament formations were in the apex and lateral epithelium of CVP forming region (Fig. 4L). These results suggested that there would be significant regulations of Shh through Wnt11 and ROCK1 to form the actin filament for proper CVP morphogenesis and pattern formation of CVP epithelium. Especially based on the similar results from the Shh gain and loss of function, there would be a negative feedback mechanism in Shh signalling during CVP development.

In order to define the precise morphological changes of epithelium in CVP formation, we measured both width of CVP apex and depth of trench wall after all experiments examined in this study. Width of CVP apex showed the interesting result after treatment of Y27632, a ROCK1 inhibitor, with the significant decreased width of CVP apex. In contrast to this analysis, the depth of the trench wall was increased in a dramatic manner after Y27632 treatment. After the experiments of gain and loss of function in Shh similar alteration patterns showed a decrease of trench wall depth (Fig. 5). These results suggested that ROCK1 would govern the shape of CVP apex region through the actin filament formation and Shh would play important roles in VEG formation.

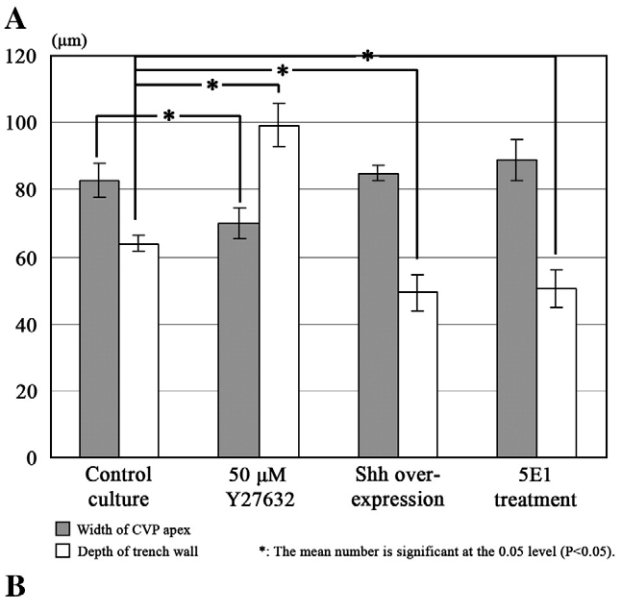

B

	Control culture (N=10)	50 μM Y27632 (N=10)	Shh over-expression (N=10)	5E1 treatment (N=10)
Width of CVP apex (μm)	82.8	69.9	84.9	88.8
S.D. (±)	4.9	4.5	2.2	6.2
Depth of trench wall (μm)	64.0	99.2	49.3	50.5
S.D. (±)	6.3	5.3	5.7	4.9

Fig. 5. Width of CVP apex and depth of trench wall were measured. Morphological alteration pattern of CVP was examined after Y27632, Shh over-expression, and 5E1 treatment. The measurement of CVP was assessed in at least 10 samples. Data are expressed as mean±SD.

Discussions

CVP development in mice embryogenesis

In the cellular level, CVP showed dynamic morphological changes such as contraction and proliferation in CVP-forming epithelium during morphogenesis (Jaskoll et al., 2004; Lee et al., 2006). Cell contractions mediated by actin–myosin complexes can have morphogenetic effects on neighboring cells and the tissue as a whole (Keller et al., 2002). Contractions of tissues during development are thought to trigger shape change and determine the character of the morphological outcomes. In a planar epithelium contraction can also lead to buckling, and thus invaginations shown in CVP morphogenesis (Jitpukdeebodintra et al., 2002). The processes surrounding this mutual induction require coordination of a complicated set of morphogenetic events, which require, among other things, rearrangements in the organization and/or function of the actin-based cytoskeleton (Bush et al., 2004; Stuart et al., 2003), rearrangements modulated by members of a family of small Rho-GTPases, namely Rac, Rho, and Cdc42 (Bishop and Hall, 2000; Tapon and Hall, 1997; Zigmond, 1996). Based on our results at E13.5 and E15.5, the specific expression patterns of *Wnt11, Shh* and ROCK1 would suggest that these signalling molecules and inner cellular component would play important roles in epithelial folding for CVP morphogenesis (Fig. 1).

Wnt signalling and cytoskeletons in CVP morphogenesis

Wnt signalling, which would be involved in formation of the cytoskeleton through ROCK modulations, was reported that play an

important role in initiation of epithelial morphogenesis (Keller et al., 2002). In addition, previous reports showed that RhoA acts downstream of *Wnt11* to regulate convergence and extension movements by involving effectors Rho kinase (Zhu et al., 2006). These reports suggested that *Wnt11* signaling would govern the cytoskeletal structures in the epithelium and pattern formation during organogenesis.

In addition, previous studies in gustatory papillae development showed interesting results of Wnt in fungiform papillae development (Iwatsuki et al., 2007; Liu et al., 2007). Based on this signalling cascade, we examined the precise molecular mechanisms of *Wnt11* and ROCK in CVP development using pharmacological inhibitor, Y27632 (Fig. 3). Various concentrations were examined using a modified rolling *in vitro* organ culture system introduced in the previous studies (Kim et al., 2003; Shiota et al., 1990). E13.5 and E15.5 were critical developmental stages for elucidating the morphogenesis of CVP, since the epithelial thickening of CVP was observed at E13.5 and the invaginations of epithelium were observed at E15.5 (Lee et al., 2006) (Fig. 1). 50 μM of Y27632 examined as the most effective concentration altered morphogenesis of CVP obviously after 2 days cultivations. The apex region of CVP forming region was much decreased but the lateral trench wall epithelium of CVP forming region was much increased (Fig. 3). These results implied that blocking of Wnt signalling by inhibiting ROCK1 would induce the Shh signalling pathway that would promote the branching morphogenesis of von Ebner's gland, which will develop after the invaginations of epithelium to form CVP. This result would coincided with a previous study in kidney ureteric bud formation (Meyer et al., 2006). As we expected actin filament formation in apex epithelium, which would play an important role to form the dome-like structure of CVP, was much decreased after Y27632 treatment (Fig. 3).

Shh signalling and cell proliferations in CVP development

Since Wnt signalling through ROCK1 showed dramatic changes in lateral trench wall forming epithelium, we examined the precise relationships among *Wnt11,* ROCK1 and *Shh*, which expressed with the specific patterns in CVP development, after Shh gain and loss of function examinations (Fig. 4). *Shh* expression is involved in the induction and morphogenesis of early CVP and salivary gland development (Jaskoll et al., 2004; Lee et al., 2006). The intensity of *Shh* expressions appear to increase in the epithelium of the lateral trench wall (where taste buds eventually form) and also in the VEG-forming area in early development (Lee et al., 2006). In mammals, taste buds are maintained by the continuous turnover of cells via cell proliferation and differentiation, together with Shh expression (Miura et al., 2003).

Functions of Shh signalling in CVP morphogenesis were analyzed using Shh over-expression and 5E1, SHH-antibody, treatment (Fig. 4). Interesting morphological changes were observed after Shh over-expression and 5E1 treatment. 5E1 treatment showed decreased invaginations level of lateral trench wall forming region of CVP in the most of cases. In addition, over-expression of Shh showed the similar morphogenesis of CVP compared with the 5E1 treatment. These results suggested that gain of function using Shh over-expression would be resulted in negative feedback to reduce the Shh expression and cell proliferation rate in VEG forming epithelium (Fig. 4H). These Shh mechanisms would be similar to previous report in lung morphogenesis (Chuang et al., 2003). In addition, Shh loss of function using 5E1, SHH-antibody, would be fatal for invagination of epithelium to form a lateral trench wall and VEG forming epithelium. Although *in vitro* rolling culture system has a limitation of nerve factors, known as one of the major factors for *Shh* expression in a previous study (Miura et al., 2001), Shh expression would play an important role in both cell proliferation of tongue epithelium and

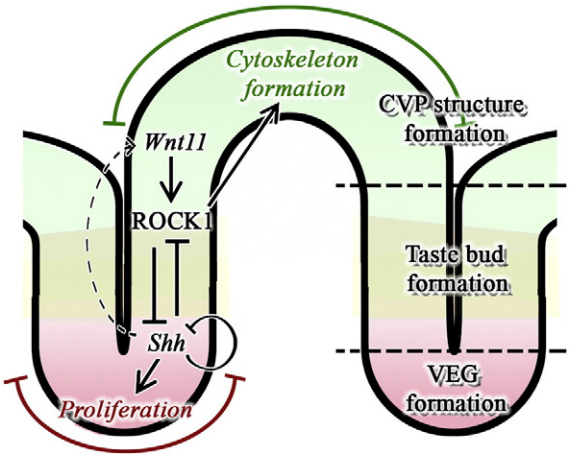

Fig. 6. Schematic diagram of Wnt11/ROCK1 and Shh signalling in epithelial morphogenesis of CVP. Invaginations of lateral trench wall forming epithelium would be governed by serial expression of Wnt11/ROCK1 and Shh signalling. Furthermore, apex epithelium and lateral epithelium would be regulated with different signalling mechanisms. In the apex epithelium of CVP, Wnt11 and ROCK1 modulate cytoskeleton formation for proper structure formation of CVP. In the lateral and VEG forming epithelium, Shh regulates cell proliferation for taste bud and VEG formation (the green color region indicates the modulations of Wnt11 and ROCK1 for cytoskeleton formation; red color regions demarcate Shh modulation area for cell proliferation; arrows indicate positive regulations; blunt arrows indicate negative regulations).

invaginations of epithelium to form the lateral wall via interaction with Wnt11 and ROCK1 signalling in CVP development.

Fate mapping of CVP

Expression patterns of Wnt11, ROCK1 and Shh signalling could not reveal the cell migration pattern in CVP formation. In order to understand the precise cell migration patterns in CVP development, we employed the Di.I. micro-injection method using *in vitro* rolling organ culture system. Epithelial cells with the various Di.I. micro-injected points including lateral, anterior, posterior and apex regions showed the interesting results, since those points would be important to elucidate the epithelial cell migration pattern in CVP formation. After 2 days *in vitro* organ culture, all of Di.I. micro-injected epithelial cells were not migrated into mesenchyme direction at all. These results implied that a major factor for invaginations of epithelium for VEG and lateral wall formation would be cell proliferations rather cell migrations.

Based on these results we could argue that specific expression patterns of *Shh* and *Wnt11* signalling including ROCK1 and actin filament would play important roles in CVP morphogenesis. Wnt11 signalling in apex region would be involved in formation of a dome-like structure of CVP through ROCK1 to integration of actin filament. Meanwhile Shh would be involved in invaginations of epithelium via proper cell proliferation. Statistical analysis also confirmed the roles of Shh and Wnt11 signalling via ROCK1 and actin filament (Fig. 5). These distinct localizations of Wnt11, ROCK1 and Shh signalling would be a plausible answer for pattern formation of taste buds, which only localize in the lateral wall epithelium (Fig. 6). Overall, we could conclude that invaginations of lateral wall forming epithelium would be governed by serial expression of Wnt11/ROCK1 and Shh signalling. Furthermore, the apex epithelium and lateral epithelium would be regulated with different signalling mechanisms such as Wnt11 and ROCK1 in the apex via cytoskeleton formation and Shh in the lateral epithelium and VEG formation through cell proliferation.

Acknowledgments

This work was supported by Korea Science and Engineering Foundation (KOSEF) grant funded by the Korea government (MEST) (No. R13-2003-013-05001-0).

References

Axelrod, J.D., Miller, J.R., Shulman, J.M., Moon, R.T., Perrimon, N., 1998. Differential recruitment of Dishevelled provides signaling specificity in the planar cell polarity and Wingless signaling pathways. Genes Dev. 12, 2610–2622.

Bishop, A.L., Hall, A., 2000. Rho GTPases and their effector proteins. Biochem. J. 348 (Pt 2), 241–255.

Bush, K.T., Sakurai, H., Steer, D.L., Leonard, M.O., Sampogna, R.V., Meyer, T.N., Schwesinger, C., Qiao, J., Nigam, S.K., 2004. TGF-beta superfamily members modulate growth, branching, shaping, and patterning of the ureteric bud. Dev. Biol. 266, 285–298.

Choi, S.C., Han, J.K., 2002. *Xenopus* Cdc42 regulates convergent extension movements during gastrulation through Wnt/Ca2+ signaling pathway. Dev. Biol. 244, 342–357.

Chuang, P.T., Kawcak, T., McMahon, A.P., 2003. Feedback control of mammalian Hedgehog signaling by the Hedgehog-binding protein, Hip1, modulates Fgf signaling during branching morphogenesis of the lung. Genes Dev. 17, 342–347.

Chuong, C.M., Patel, N., Lin, J., Jung, H.S., Widelitz, R.B., 2000. Sonic hedgehog signaling pathway in vertebrate epithelial appendage morphogenesis: perspectives in development and evolution. Cell Mol. Life Sci. 57, 1672–1681.

Dale, T.C., 1998. Signal transduction by the Wnt family of ligands. Biochem. J. 329 (Pt 2), 209–223.

Eblaghie, M.C., Song, S.J., Kim, J.Y., Akita, K., Tickle, C., Jung, H.S., 2004. Interactions between FGF and Wnt signals and Tbx3 gene expression in mammary gland initiation in mouse embryos. J. Anat. 205, 1–13.

Habas, R., Dawid, I.B., He, X., 2003. Coactivation of Rac and Rho by Wnt/Frizzled signaling is required for vertebrate gastrulation. Genes Dev. 17, 295–309.

Hartmann, C., Tabin, C.J., 2000. Dual roles of Wnt signaling during chondrogenesis in the chicken limb. Development 127, 3141–3159.

He, X., Saint-Jeannet, J.P., Wang, Y., Nathans, J., Dawid, I., Varmus, H., 1997. A member of the Frizzled protein family mediating axis induction by Wnt-5A. Science 275, 1652–1654.

Huelsken, J., Birchmeier, W., 2001. New aspects of Wnt signaling pathways in higher vertebrates. Curr. Opin. Genet. Dev. 11, 547–553.

Iwatsuki, K., Liu, H.X., Gronder, A., Singer, M.A., Lane, T.F., Grosschedl, R., Mistretta, C.M., Margolskee, R.F., 2007. Wnt signaling interacts with Shh to regulate taste papilla development. Proc. Natl. Acad. Sci. U. S. A. 104, 2253–2258.

Jaskoll, T., Leo, T., Witcher, D., Ormestad, M., Astorga, J., Bringas Jr., P., Carlsson, P., Melnick, M., 2004. Sonic hedgehog signaling plays an essential role during embryonic salivary gland epithelial branching morphogenesis. Dev. Dyn. 229, 722–732.

Jitpukdeebodintra, S., Chai, Y., Snead, M.L., 2002. Developmental patterning of the circumvallate papilla. Int. J. Dev. Biol. 46, 755–763.

Keller, H., Rentsch, P., Hagmann, J., 2002. Differences in cortical actin structure and dynamics document that different types of blebs are formed by distinct mechanisms. Exp. Cell Res. 277, 161–172.

Kim, J.Y., Mochizuki, T., Akita, K., Jung, H.S., 2003. Morphological evidence of the importance of epithelial tissue during mouse tongue development. Exp. Cell Res. 290, 217–226.

Kim, J.Y., Cho, S.W., Lee, M.J., Hwang, H.J., Lee, J.M., Lee, S.I., Muramatsu, T., Shimono, M., Jung, H.S., 2005a. Inhibition of connexin 43 alters Shh and Bmp-2 expression patterns in embryonic mouse tongue. Cell Tissue Res. 320, 409–415.

Kim, J.Y., Cho, S.W., Song, W.C., Lee, M.J., Cai, J., Ohk, S.H., Song, H.K., Degan, A., Jung, H.S., 2005b. Formation of spacing pattern and morphogenesis of chick feather buds is regulated by cytoskeletal structures. Differentiation 73, 240–248.

Kuhl, M., Sheldahl, L.C., Park, M., Miller, J.R., Moon, R.T., 2000. The Wnt/Ca2+ pathway: a new vertebrate Wnt signaling pathway takes shape. Trends Genet. 16, 279–283.

Lamm, M.L., Catbagan, W.S., Laciak, R.J., Barnett, D.H., Hebner, C.M., Gaffield, W., Walterhouse, D., Iannaccone, P., Bushman, W., 2002. Sonic hedgehog activates mesenchymal Gli1 expression during prostate ductal bud formation. Dev. Biol. 249, 349–366.

Lee, M.J., Kim, J.Y., Lee, S.I., Sasaki, H., Lunny, D.P., Lane, E.B., Jung, H.S., 2006. Association of Shh and Ptc with keratin localization in the initiation of the formation of circumvallate papilla and von Ebner's gland. Cell Tissue Res. 325, 253–261.

Liu, F., Thirumangalathu, S., Gallant, N.M., Yang, S.H., Stoick-Cooper, C.L., Reddy, S.T., Andl, T., Taketo, M.M., Dlugosz, A.A., Moon, R.T., Barlow, L.A., Millar, S.E., 2007. Wnt-beta-catenin signaling initiates taste papilla development. Nat. Genet. 39, 106–112.

Meyer, T.N., Schwesinger, C., Sampogna, R.V., Vaughn, D.A., Stuart, R.O., Steer, D.L., Bush, K.T., Nigam, S.K., 2006. Rho kinase acts at separate steps in ureteric bud and metanephric mesenchyme morphogenesis during kidney development. Differentiation 74, 638–647.

Michael, L., Sweeney, D.E., Davies, J.A., 2005. A role for microfilament-based contraction in branching morphogenesis of the ureteric bud. Kidney Int. 68, 2010–2018.

Miura, H., Kusakabe, Y., Sugiyama, C., Kawamatsu, M., Ninomiya, Y., Motoyama, J., Hino, A., 2001. Shh and Ptc are associated with taste bud maintenance in the adult mouse. Mech. Dev. 106, 143–145.

Miura, H., Kusakabe, Y., Kato, H., Miura-Ohnuma, J., Tagami, M., Ninomiya, Y., Hino, A., 2003. Co-expression pattern of Shh with Prox1 and that of Nkx2.2 with Mash1 in mouse taste bud. Gene Expr. Patterns 3, 427–430.

Nusse, R., Varmus, H.E., 1992. Wnt genes. Cell 69, 1073–1087.

Pispa, J., Thesleff, I., 2003. Mechanisms of ectodermal organogenesis. Dev. Biol. 262, 195–205.

Shiota, K., Kosazuma, T., Klug, S., Neubert, D., 1990. Development of the fetal mouse palate in suspension organ culture. Acta. Anat. (Basel) 137, 59–64.

Stuart, R.O., Bush, K.T., Nigam, S.K., 2003. Changes in gene expression patterns in the ureteric bud and metanephric mesenchyme in models of kidney development. Kidney Int. 64, 1997–2008.

Tapon, N., Hall, A., 1997. Rho, Rac and Cdc42 GTPases regulate the organization of the actin cytoskeleton. Curr. Opin. Cell Biol. 9, 86–92.

Thibert, C., Teillet, M.A., Lapointe, F., Mazelin, L., Le Douarin, N.M., Mehlen, P., 2003. Inhibition of neuroepithelial patched-induced apoptosis by sonic hedgehog. Science 301, 843–846.

Winklbauer, R., Medina, A., Swain, R.K., Steinbeisser, H., 2001. Frizzled-7 signalling controls tissue separation during *Xenopus* gastrulation. Nature 413, 856–860.

Yu, J., Carroll, T.J., McMahon, A.P., 2002. Sonic hedgehog regulates proliferation and differentiation of mesenchymal cells in the mouse metanephric kidney. Development 129, 5301–5312.

Zhu, S., Liu, L., Korzh, V., Gong, Z., Low, B.C., 2006. RhoA acts downstream of Wnt5 and Wnt11 to regulate convergence and extension movements by involving effectors Rho kinase and *Diaphanous*: use of zebrafish as an in vivo model for GTPase signaling. Cell Signal 18, 359–372.

Zigmond, S.H., 1996. Signal transduction and actin filament organization. Curr. Opin. Cell Biol. 8, 66–73.